

Design concepts for an improved integrated scanning SQUID

Nicholas C. Koshnick

Center for Probing the Nanoscale, Stanford University, Stanford, CA 94305

E-mail: koshnick@alum.dartmouth.org

John R. Kirtley

Center for Probing the Nanoscale, Stanford University, Stanford, CA 94305

E-mail: kirtley@ucsbalum.net

Kathryn A. Moler

Center for Probing the Nanoscale, Stanford University, Stanford, CA 94305

E-mail: kmoler@stanford.edu

Abstract. In this paper we discuss design concepts for increasing the spatial resolution, improving the sensitivity, and reducing the invasiveness in scanning Superconducting Quantum Interference Device (SQUID) microscope sensors with integrated flux pickup loops. This can be done not only by reducing the ground-rule line widths and spacings, but also by taking advantage of planarization, reducing flux noise through reducing the SQUID inductance, and reducing back-action through dispersive readouts or on-chip filtering.

PACS numbers: 85.25.Dq, 85.25.Am

1. Introduction

Scanning SQUID microscope sensors with integrated flux pickup loops [1, 2] can have several advantages over sensors composed solely of very small SQUIDs: they can have reduced interaction with the sample because the junctions can be physically distant from the sample, it is possible to make very small, well shielded pickup loops without having to make the entire device small, and it is comparatively easy to flux modulate them. However, integrated SQUID sensors have the disadvantage of higher complexity, since they require crossovers and overlays for good shielding of the leads to the pickup loop. Integrated SQUID sensors have been very successful in, for example, elucidating the pairing symmetry in the cuprate high temperature superconductors [3, 4], testing the interplane tunneling model for the mechanism of high temperature superconductivity [5], and imaging spontaneous circulating currents in mesoscopic normal metal rings [6]. Further, integrated SQUID sensors can be designed in a susceptometer configuration, with a field coil surrounding the pickup loop [7]. This allows for strong discrimination against background fields [6, 8], manipulation of local magnetic features [7, 9], and such measurements as imaging of the local superfluid density of a superconductor [10]. It is important to minimize the size of the pickup loop and the spacing between the loop and the sample, while maintaining good shielding of the leads to the pickup loop, to optimize sensor spatial resolution and sensitivity.

In previous work [11, 12], we presented SQUID susceptometers that were designed explicitly for the purpose of measuring mesoscopic objects. The first paper in this series [11] focused on the design's symmetry and on issues relating to operation and performance. The primary achievement of this generation of devices is the ability to measure the magnetic signals from micron-sized objects down to the fundamental Johnson noise limits [6]. The second paper in this series [12] focussed on reducing the pickup loop size and line width to a point close to the limits set by the superconducting penetration depth of Niobium, the material of choice for superconducting integrated circuits. This paper also demonstrated a design that avoids the thickness problems associated with the multiple layers required by a shielded device with a pickup loop inside a larger field coil. Specifically, layer crossings occurred in such a way that the pickup loop could be positioned as close as possible to the surface (Fig 1a).

In this work, we discuss additional ways to improve SQUIDs for the purpose of measuring mesoscopic objects as well as imaging. This revision was motivated, in part, by the possibility of a planarized superconducting process [13], with design rules that allow for 250 nm optically defined features, and 1 μm vias. Section 2 discusses design improvements that would be made possible if this process is implemented. Planarization allows for significantly reduced geometric constraints in the tip design, and continuous conducting layers that reduce vortex motion, thereby allowing for higher locally applied fields. The small feature size allows for a significant reduction in the primary imaging area and in the device's stray pickup area. Section 3 outlines steps that would reduce the SQUID's inductance below that of previous designs. This in turn should allow for a

reduction in the SQUID's flux noise. The most significant reduction in inductance comes from a lower-inductance modulation loop area, and a flux-coupled, single pickup loop design that replaces previous designs, which were direct-coupled and had two pickup loops. The final section, section 4, describes methods for reducing the amount of Johnson noise seen by the sample, thus allowing for lower sample temperatures and the possibility of measuring additional mesoscopic effects in small samples.

2. Advantages of a planarized device with multi-layer sub-micron features

The thickness of superconducting layers in an integrated process is constrained to be larger than the superconducting penetration depth. Layers thinner than this have limited field screening abilities and narrow, thin features can have a non-negligible kinetic inductance. To avoid these potential problems, superconducting foundries post design rules with layer thicknesses between 150 and 200 nm, substantially greater than the approximately 85 nm penetration depth of sputtered Niobium. Given the thickness of individual layers, it is difficult to design deep sub-micron features into a multi-layered architecture, because small features cannot be reliably fabricated when the underlying height profile varies on the same length scale. It is therefore reasonable to conclude that any new superconducting foundry that utilizes the now readily available sub-micron lithography tools, will also likely choose to adopt chemical-mechanical polishing steps after each conductor/insulator layer.

The adoption of a planarization process would considerably reduce the geometric constraints that determine whether the pickup loop layer will touch down first. Our previous paper [12] described the use of a shallow etch outside the pickup loop and a deep etch outside the field coil. This geometry, shown in the layer diagram in Fig. 1a, can allow a top-layer pickup loop to touch down first with an alignment tolerance of 3 degrees. Such alignment tolerance is necessary because of the limited alignment ability in hand-crafted scanners and because changes after alignment due to thermal contractions. With a planarized process, a minimum alignment angle is no longer inherent in the design. This means a larger tolerance angle can be achieved (Fig 1b,c), or a wider field coil can be used, which has the potential of increasing the maximum usable applied field.

Another very important geometric advantage of a planarized design is that the via to a top layer pickup loop can be much closer to the pickup loop itself, which would allow for a smaller imaging kernel. In the design shown in Fig 1a, the electrical connection to the top layer is more than 15 μm from the touch down point. Although the magnetic field seen by the pickup loop leads (in layer W2) is partially screened by the middle layer (W1), the long leads still make for a large area where the SQUID is responsive to the sample's magnetic field. In a planarized design, the vias can be brought as close as is allowed by the design rules.

In previous papers we have demonstrated how susceptometry and background cancellations can enable Johnson noise limited detection of magnetic signals from

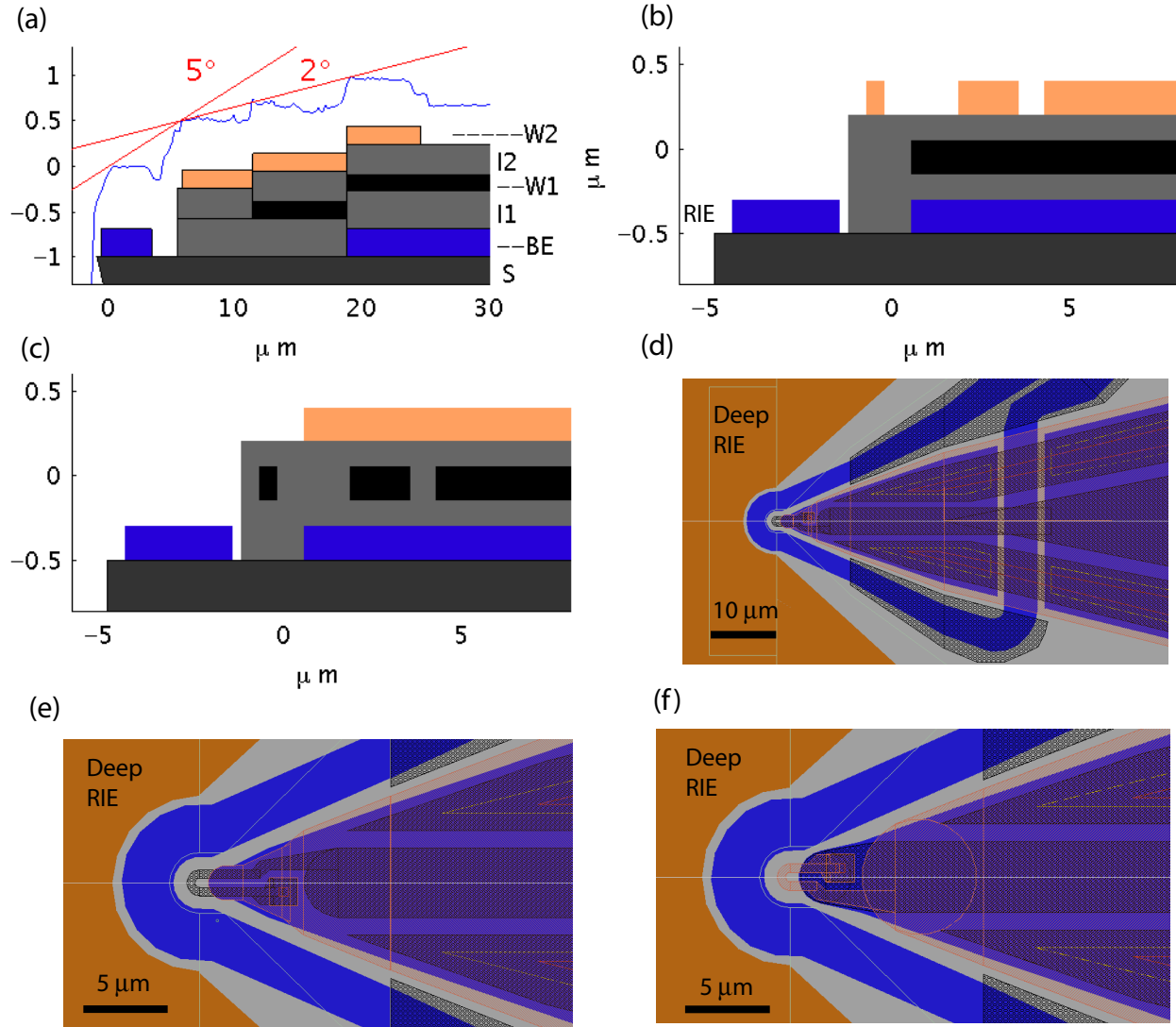


Figure 1. (Color Online) Comparison of design layouts and layer considerations for a planarized vs a non-planarized design with sub-micron feature sizes. (a-c) Cross-sections down the the center line of the design showing layer thickness effects. (a) Layer thicknesses of a non planarized process described elsewhere [12], with three superconducting layers (BE, W1, W2), two insulating layers (I1, I2), and the substrate. Atomic force microscope data (blue) shows the tolerance angles that would allow a top layer FIB fabricated pickup loop to touch first. (b) The layer thicknesses of a planarized design allow for much shorter pickup loop leads with the same tolerance angles. (c) The layer thickness diagram of a middle layer pickup loop design. (d-f) Top down view of SQUID design. (d) Passing the field coil under the linear coax section of the SQUID leads allows for a symmetric tip. (e) The mid-layer pickup loop design shown in (c). (f) The top layer design shown in (b).

mesoscopic samples such as superconducting and normal metal rings. Such objects can have periodic response due to quantum mechanical effects, where the amplitude of this response is inversely related to the ring size. The minimum ring size is set by the applied field, because at least half a flux quantum of field is required to distinguish a periodic signal from an (often much larger) linear signal related to spins [14]. Furthermore, we have found that if the field is not sourced by the local field coils, then coupling into the SQUID modulation loop, SQUID array amplifier, and additional vibration-related signals severely reduce the technique's sensitivity. Increasing the width and thickness of the field coil loop is not enough to increase the usable maximum applied field. We have found that these measures increase the field coil current that makes the SQUID go normal, but that sensitivity is no longer optimal once vortices begin to move at a much lower field [12]. Planarization allows for continuous conducting layers, which reduces thin superconducting areas in the design, and thus should help to reduce the field coil current where vortices begin to move.

Spatial resolution is an important factor of a SQUID's design for many reasons. In the large set of cases where it is acceptable to have the pickup loop $\gtrsim 300$ nm from the sample, it is advantageous to put the pickup loop in the middle layer as shown in Figs. 1c-e. This allows for a minimal image kernel size, because both the top and bottom layers can screen the pickup loop from magnetic field. The width of the shielding layers has been kept to a minimum in the area immediately adjacent to the pickup loop to minimize the flux-focusing effects that can increase the effective pickup loop size [1].

Our design for a SQUID with a pickup loop in the top layer, Fig. 1f, is similar to that of Fig. 1e, except that the flux-focusing condition was relaxed to allow for shorter leads and thus less stray coupling. Both designs have a field coil line that crosses far behind the pickup loop area in a region where the SQUID has a linear coaxial geometry, Fig. 1d. This allows for a symmetric tip, minimal unshielded leads, and thus a pickup and transition area that contributes minimally to the inductance of the rest of the design.

3. Optimizing flux sensitivity through reduced inductance

While our previous devices have flux sensitivities that are comparable to or better than scanning devices of their kind, quantum-limited devices [15] with flux sensitivities as low as $\sim 0.08\mu\Phi_0/\sqrt{Hz}$ [16] have been realized. We note that our designs are limited by thermal noise in the shunt resistors. When optimally tuned, this Johnson noise dependence scales like $L^{3/2}$ where L is the SQUID's self inductance [17]. An optimally designed quantum limited flux noise scales as $L^{1/2}$. By reducing L one can both reduce the SQUID's overall white noise floor, and increase the temperature, where temperature-independent quantum noise becomes the dominate noise source.

For both the optically [11] and FIB [12] fabricated SQUIDs, the inductance [18] of each section is approximately 12 pH per pickup loop, 10 pH/mm in the linear coaxial connection region, and ~ 55 pH for the core junction/modulation loop area.

The majority of the core area inductance in the previous designs come from the

two modulation loops, each with an inner diameter of $10\text{ }\mu\text{m}$. Estimating from their inner diameter [19], these two loops contribute 30 pH to the total inductance. This contribution would decrease linearly with a reduction in the diameter of the loop. The main drawback to this change in our case (low bandwidth requirements) is that more modulation-loop current would be required to keep the SQUID in a flux-locked loop. Increases in the amount of current sent to the modulation loops can lead to heating from stray resistances in dilution refrigerator temperature wiring. Reducing the modulation loop diameter to $4\text{ }\mu\text{m}$ decreases the self inductance to 12 pH , while maintaining a reasonable $175\text{ }\mu\text{A}/\phi_0$ mutual inductance. Further enhancement could come from having only one modulation loop in a non-gradiometric design. Small modulation loops with multiple windings could also allow for smaller loops.

Another avenue worth considering for reduced inductance involves questioning the assumption that dual, counter wound pickup coils aid background subtraction. Assuming that comparative/background measurements are made, either by scanning or by systematically positioning the sensor at various points around a mesoscopic object, the net effect of the counter winding is to reduce the pickup loop coupling to the field coils to a sufficient extent that the dynamic range of the direct signal does not overwhelm the room temperature electronics. For small pickup loops the field coil coupling is already small, thus the counter-winding may not be necessary. It is also physically reasonable to require room temperature electronics that send some of the field coil signal to the modulation loop, so that this direct coupled signal is cancelled before amplification. It is thus possible that a one-sided SQUID could have lower noise.

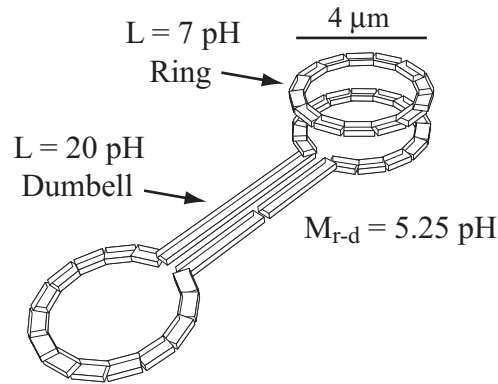


Figure 2. A simplified model for a flux coupled SQUID, which consists of a dumbbell shaped flux coupler with $4\text{ }\mu\text{m}$ loops, and a $4\text{ }\mu\text{m}$ ring with specified inductances.

Directly cutting out one of the pickup loops creates an unbalanced inductance in the two sides of the SQUID circuit. This leads to non-symmetric I-V characteristics [20] and slightly more complicated modeling, but does not necessarily reduce the flux sensitivity. One way to reduce the unbalanced inductance problem would be to remove the modulation loops all together. In the resulting two-pickup loop structure, the non-scanning pickup loop could be associated with an additional field coil that acts as a modulation loop.

An alternative design direction is to change the bulk of the current design into a flux coupler with just the central part being an independent low-inductance SQUID. A simplified Fasthenry [18] model of superconducting elements (Fig 2) illustrates the tradeoffs between the reduced coupling to the sample, and the reduction in the SQUID's inductance. It considers the inductances of two objects: a simple $4\ \mu\text{m}$ diameter ring, and a “dumbbell” consisting of two $4\ \mu\text{m}$ diameter loops coupled by two lines. This dumbbell object has a self inductance, $L_d = 20\ \text{pH}$, and can be considered either as a direct coupled SQUID or the flux coupler that is coupled to the ring. In the latter case, the ring, which has a self inductance $L_r = 7\ \text{pH}$, represents the non-directly coupled SQUID. The mutual inductance between the ring and dumbbell is $M_{r-d} = 5.25\ \text{pH}$. The flux-coupled SQUID only sees $M_{r-d}/L_d = .26$ as much flux as its direct-coupled counterpart, but when limited by Johnson noise, it has $(L_r/L_d)^{3/2} = .21$ as much white noise. Flux-coupled and direct-coupled SQUIDs therefore have very similar white noise characteristics until the inductance is small enough that the $L^{1/2}$ -dependent quantum limit is applicable. The main advantage may be that a flux-coupled SQUID could have only one pickup loop, substantially reducing the inductance without leaving the SQUID unbalanced.

4. Reducing SQUID sample back action

Understanding the way the SQUID perturbs the sample is an important part of measuring quantum effects in mesoscopic samples. We will consider one of the simplest kinds of back action on the sample, joule heating from SQUID radiation at the Josephson frequency, f_j . While studying persistent currents in normal metal rings, we discovered that metallic regions had a spin-like linear susceptibility that increased with decreasing temperature [14]. The coupled SQUID radiation of $\approx 10^{-14}$ Watts for our $R \approx 2\Omega$ rings, balanced by electron-phonon limited cooling [21], limited the temperature in isolated rings to about 200 mK [6]. Since there are many interesting effects that only occur below this temperature, it is important to consider design aspects that can reduce this form of back action.

In general, the cost of reduced back-action is often reduced sensitivity. A simple estimate for the energy dissipated in a ring is given by the flux-change-induced ring-voltage

$$V_{ring} = \frac{d\Phi}{dt} = I_0 f_j M_{SQ-s} \quad (1)$$

where M_{SQ-s} is the mutual inductance between the SQUID and the sample. The power dissipated is then just V_{ring}^2/R , where R is the ring's resistance. One can reduce this heating effect by moving the SQUID further away from the sample, thereby reducing M_{SQ-s} . This is only a useful approach when there is ample signal. Another approach is to bias the SQUID with the lowest possible voltage, and thus lowest operating f_j . In general, this approach is limited by the minimum voltage bias ($\propto k_B T/e$), where the

SQUID noise begins to deteriorate, and by the feedback electronics' ability to lock into a signal that has a reduced modulation amplitude.

The noise dependance on $L^{3/2}$, mentioned in section 3, was calculated in the $\beta_L = 2LI_0/\Phi_0 \approx 1$ limit, where the standard design rules [17] set critical current to $I_0 = \Phi_0/2L$, and the appropriate shunt resistor is determined by $\beta_c \approx 1$. Increasing the flux sensitivity by reducing L thus comes with an increased I_0 and correspondingly increased radiation on the sample. While the SQUID's energy sensitivity, Φ_n^2/L , is optimal for $\beta_L \approx 1$, the relevant figure of merit when measuring mesoscopic samples must include back action. The optimal point in this case would probably require $I_0 < \Phi_0/2L$. This effect has been analyzed in quantum limited SQUIDs [22].

Another way to reduce the back action on the sample is to read out the SQUID dispersively. Josephson radiation (and thus sample heating) does not occur when the SQUID is in the zero voltage state. Dispersive readout measures the flux-dependence of the inductance, without inducing voltage, typically by placing the SQUID in some kind of resonant circuit. Thus the Josephson radiation (of typically 1-10 GHz) gets replaced by the readout frequency (~ 100 Mhz). One excellent way to implement dispersive readout involves the microstrip SQUID amplifier designed by the group of John Clarke [23]. The superconducting qubit community has invested considerable effort in comparing the back action from this type of measurement to the back action from other non-voltage state readout schemes, such as the scanning SQUIDs [24] that rely on the bias current switching threshold.

A final way to limit SQUID heating would be to implement on-chip filters inside the SQUID circuit that divert the Josephson frequency currents from the pickup loop and sample. This approach was implemented with LC filters by John Price's group [25] in a two-chip design. Implementing the same type of LC filters on a single chip would help to keep inductive losses to a minimum. We note the capacitance in our 40 μm wide, 1.2 mm long linear coaxial coupler with a 200 nm wire-to-wire spacing is roughly 20 pF. The 30 pH pickup loop and strip line inductance thus has a cutoff frequency of 6.5 GHz, indicating that a reasonable portion of the Josephson frequency current is already not flowing through the pickup loop itself. We therefore believe that further design work that explicitly exploits this effect could have significant success.

A second type of on-chip filter involves placing a small (0.3Ω) shunting resistor between the SQUID and the pickup loop. This form of RC filter works as a frequency dependent current divider, where the Josephson frequency currents would see a reactance of 0.95Ω (15 pH at ~ 10 GHz) and thus largely run through the shunt, whereas the zero frequency currents that set up the SQUID phase relations would still all be coupled to the pickup loop itself.

As with the LC filter technique, this line of reasoning intrinsically relies on the fact that we are trying to measure time-averaged equilibrium currents in our rings, and thus can simply limit the frequencies where effective coupling occurs to some value below the frequencies involved with the intrinsic SQUID and sample dynamics. The LC filter could effectively shunt the great majority of the Josephson frequency radiation if an additional

high capacitance layer, with sufficiently low stray inductance, was incorporated into the superconducting process. The effectiveness of the RC filter is limited by the Johnson current noise it sends through the pickup loop, integrated up to the bandwidth set by the LC filter. In practice, however, it is likely that this RC shunting technique could reduce the sample temperature significantly before this limit sets in.

This work was supported by NSF Grants Nos. DMR-0803974 and PHY-0425897

References

- [1] M. B. Ketchen and J. R. Kirtley. Design and performance aspects of pickup loop structures for miniature squid magnetometry. *IEEE Transactions on Applied Superconductivity*, 5(2):2133 – 2136, Jun 1995.
- [2] J. R. Kirtley, M. B. Ketchen, K. G. Stawiasz, J. Z. Sun, W. J. Gallagher, S. H. Blanton, and S. J. Wind. High-resolution scanning squid microscope. *Applied Physics Letters*, 66:1138–1140, February 1995.
- [3] C. C. Tsuei, J. R. Kirtley, C. C. Chi, L. S. Yu-Jahnes, A. Gupta, T. Shaw, J. Z. Sun, and M. B. Ketchen. Pairing symmetry and flux quantization in a tricrystal superconducting ring of $\text{YBa}_2\text{Cu}_3\text{O}_{7-\delta}$. *Physical review letters*, 73(4):593–596, 1994.
- [4] J.R. Kirtley, C.C. Tsuei, Ariando, C.J.M. Verwijs, S. Harkema, and H. Hilgenkamp. Angle-resolved phase-sensitive determination of the in-plane gap symmetry in $\text{YBa}_2\text{Cu}_3\text{O}_{7-\delta}$. *Nature Physics*, 2:190, 2006.
- [5] Kathryn A. Moler, John R. Kirtley, D. G. Hinks, T. W. Li, and Ming Xu. Images of interlayer josephson vortices in $\text{Tl}_2\text{Ba}_2\text{CuO}_{6+\delta}$. *Science*, 279(5354):1193–1196, February 1998.
- [6] Hendrik Bluhm, Nicholas C. Koshnick, Julie A. Bert, Martin E. Huber, and Kathryn A. Moler. Persistent currents in normal metal rings. *Physical Review Letters*, 102(13):136802–4, April 2009.
- [7] Brian W. Gardner, Janice C. Wynn, Per G. Bjornsson, Eric W. J. Straver, Kathryn A. Moler, John R. Kirtley, and Mark B. Ketchen. Scanning superconducting quantum interference device susceptometry. *Review of Scientific Instruments*, 72(5):2361–2364, 2001.
- [8] Nicholas C. Koshnick, Hendrik Bluhm, Martin E. Huber, and Kathryn A. Moler. Fluctuation superconductivity in mesoscopic aluminum rings. *Science*, 318:1440–1443, November 2007.
- [9] Hans Hilgenkamp, Ariando, Henk-Jan H. Smilde, Dave H. A. Blank, Guus Rijnders, Horst Rogalla, John R. Kirtley, and Chang C. Tsuei. Ordering and manipulation of the magnetic moments in large-scale superconducting π -loop arrays. *Nature*, 422(6927):50–53, March 2003.
- [10] F Tafuri, J R Kirtley, P G Medaglia, P Orgiani, and G Balestrino. Magnetic imaging of pearl vortices in artificially layered $(\text{Ba}_{0.9}\text{Nd}_{0.1}\text{CuO}_{2+x})_m/(\text{CaCuO}_2)_n$ systems. *Physical Review Letters*, 92(15):157006, April 2004. PMID: 15169312.
- [11] Martin E. Huber, Nicholas C. Koshnick, Hendrik Bluhm, Leonard J. Archuleta, Tommy Azua, Per G. Björnsson, Brian W. Gardner, Sean T. Halloran, Erik A. Lucero, and Kathryn A. Moler. Gradiometric micro-squid susceptometer for scanning measurements of mesoscopic samples. *Review of Scientific Instruments*, 79(5):053704, 2008.
- [12] Nicholas C. Koshnick, Martin E. Huber, Julie A. Bert, Clifford W. Hicks, Jeff Large, Hal Edwards, and Kathryn A. Moler. A terraced scanning superconducting quantum interference device susceptometer with submicron pickup loops. *Applied Physics Letters*, 93(24):243101–3, December 2008.
- [13] M. B. Ketchen, D. Pearson, A. W. Kleinsasser, C.-K. Hu, M. Smyth, J. Logan, K. Stawiasz, E. Baran, M. Jaso, T. Ross, K. Petrillo, M. Manny, S. Basavaiah, S. Brodsky, S. B. Kaplan, W. J. Gallagher, and M. Bhushan. Sub- μm , planarized, Nb- AlO_x -Nb josephson process for 125 mm wafers developed in partnership with Si technology. *Applied Physics Letters*, 59(20):2609–2611, November 1991.

- [14] Hendrik Bluhm, Julie A. Bert, Nicholas C. Koshnick, Martin E. Huber, and Kathryn A. Moler. Spinlike susceptibility of metallic and insulating thin films at low temperature. *Physical Review Letters*, 103(2):026805, 2009.
- [15] J. Clarke and A. I. Braginski, editors. *The SQUID Handbook*. Weinheim : Wiley-VCH, 2003.
- [16] D. D. Awschalom, J. R. Rozen, M. B. Ketchen, W. J. Gallagher, A. W. Kleinsasser, R. L. Sandstrom, and B. Bumble. Low-noise modular microsusceptometer using nearly quantum limited dc squids. *Applied Physics Letters*, 53(21):2108–2110, November 1988.
- [17] Claudia D. Tesche and John Clarke. dc squid: Noise and optimization. *Journal of Low Temperature Physics*, 29:301–331, November 1977.
- [18] M. Kamon, M. J. Tsuk, and J. K. White. Fasthenry: a multipole-accelerated 3-d inductance extraction program. *IEEE Transactions on Microwave Theory and Techniques*, 42(9):1750 – 1758, Sept 1994.
- [19] J. Jaycox and M. Ketchen. Planar coupling scheme for ultra low noise DC SQUIDS. *Magnetics, IEEE Transactions on*, 17(1):400–403, 1981.
- [20] R. L. Peterson and C. A. Hamilton. Analysis of threshold curves for superconducting interferometers. *Journal of Applied Physics*, 50:8135–8142, December 1979.
- [21] F. C. Wellstood, C. Urbina, and John Clarke. Hot-electron effects in metals. *Physical Review B*, 49:5942, March 1994.
- [22] V. Danilov, K. Likharev, and A. Zorin. Quantum noise in squids. *Magnetics, IEEE Transactions on*, 19(3):572–575, 1983.
- [23] Michael Muck, J. B. Kycia, and John Clarke. Superconducting quantum interference device as a near-quantum-limited amplifier at 0.5 ghz. *Applied Physics Letters*, 78(7):967–969, February 2001.
- [24] K. Hasselbach, C. Veauvy, and D. Mailly. Microsquid magnetometry and magnetic imaging. *Physica C*, 332:140–147, May 2000.
- [25] X. Zhang and J. C. Price. Susceptibility of a mesoscopic superconducting ring. *Phys. Rev. B*, 55(5):3128 – 3140, FEB 1997.